

15th Water-Rock Interaction International Symposium, WRI-15

Basaluminite structure and its environmental implications

Sergio Carrero^{a,1}, Alejandro Fernandez-Martinez^{b,c}, Rafael Pérez-López^a and José Miguel Nieto^a

^aDepartment of Geology, University of Huelva, Campus 'El Carmen', 21071, Huelva, Spain

^bCNRS, ISTERre, F-38041 Grenoble, France

^cUniversité Grenoble Alpes, ISTERre, F-38041 Grenoble, France

Abstract

Basaluminite is a nanocrystalline aluminum oxyhydrogensulfate of important environmental implications. It is present in areas affected by acid mine drainage and acid sulfate soils, where potential toxic elements present in solution, such as Cu and As, can be retained by co-precipitation or adsorption onto it. Basaluminite has been described as a nanomineral variety of felsöbányaite. In the present study, high-energy X-ray diffraction (HEXD) and extended X-ray adsorption fine structure (EXAFS) experiments were performed to determine the local order of basaluminite nanoparticles. Pair distribution function (PDF) analyses showed that both synthetic and natural basaluminite have identical short-range order, with 1 nm coherent domain size. PDFs also show strong similarities between the local order of basaluminite and felsobanyaite. On the other hand, S K-edge EXAFS showed different structural coordination between natural and synthetic basaluminite, where sulfate in the natural phase were coordinated in outer-sphere positions whereas inner-sphere sulfate was observed in the synthetic samples. Preliminary results indicated that basaluminite is a highly defective felsobanyaite mineral nanoparticle. This nanocrystalline character has therefore important implication in terms of stability in natural condition and contaminant mobility in stream affected by acid sulfate water.

© 2017 The Authors. Published by Elsevier B.V. This is an open access article under the CC BY-NC-ND license

(<http://creativecommons.org/licenses/by-nc-nd/4.0/>).

Peer-review under responsibility of the organizing committee of WRI-15

Keywords: Basaluminite, felsöbányaite, Structure, PDF, EXAFS

1. Introduction

Basaluminite is the name that receives the white precipitate formed in streams affected by acid mine drainage (AMD) and in acid solid soils (ASS), with high aluminum and sulfate concentrations in solution when pH values are around 4.5¹. Basaluminite has important environmental implications since this mineral shows high affinity by

* Corresponding author. Tel.: +34-95-921-9682; fax: +34-95-921-9810.

E-mail address: Sergio.carrero@dgeo.uhu.es

potentially hazardous elements present in solution (e.g. Cu and As) in basins impacted by AMD and ASS^{2,3}. As described by⁴ basaluminite as the nanomineral variety of felsöbányaite ($\text{Al}_4(\text{OH})_{10}(\text{SO}_4)\cdot 4\text{H}_2\text{O}$), a rare mineral (space group $\text{P}2_1\text{-C}_2^2$). However, previous researches have indicated that nanoparticles may contain high levels of structural disorder that can substantially modify material properties and thus cannot solely be considered as small piece of a bulk material.⁵ On the other hand, while basaluminite has been discredited as a mineral by International Mineralogical Association (IMA), hydrobasaluminite, the hydrated variety of basaluminite, is still considered as a mineral. The main aims of the present study are: (1) to characterize the local structure of basaluminite and (2) to indicate its differences and similarities with felsöbányaite. To this end, high-energy X-ray diffraction (HEXD) and extended X-ray adsorption fine structure (EXAFS) experiments in the S K-edge were performed in natural and synthetic samples of felsöbányaite and basaluminite, in order to determine the local order and to establish the sulfate coordination in the structure.

2. Materials and methods

2.1. Solid samples

Three types of Al-phases were used in this study: natural felsöbányaite, and synthetic and natural basaluminite. A sample of natural felsöbányaite from the Felsöbányaite region (Romania) was obtained from a private collection. Natural basaluminite was obtained by slow titration under continuous stirring of an AMD solution, from the Perrunal abandoned mine (Iberian Pyrite Belt, SW Spain), with $\text{Ca}(\text{OH})_2$ 0.01 M until pH 5, removing previously the iron precipitates, as described by³. Synthetic basaluminite was prepared by drop-by-drop addition of 214 mL of a 0.015 M $\text{Ca}(\text{OH})_2$ solution to 30 mL of 0.05 M $\text{Al}_2(\text{SO}_4)_3\cdot 18\text{H}_2\text{O}$ in continuous stirring. These precipitates were washed several times with deionized and freeze-dried. After drying, the samples were digested in aqua regia for further chemical analysis.

2.2. Analytical techniques

HEXD experiments were performed at the beamline ID31 of the European Synchrotron Radiation Facility (ESRF; Grenoble, France). Powder samples were loaded into polyamide (Kapton) capillaries. Sample and background measurements were carried out at room temperature in a q -range of $0\text{-}25 \text{ \AA}^{-1}$. Incident X-rays had an energy of 69.5 KeV ($\lambda = 0.1784 \text{ \AA}$). Structure factors and pair distribution functions (PDF) were obtained using the PDFGetX3 software⁶. EXAFS data was collected for natural and synthetic basaluminite at the XAFS (11.1) beamline of the ELETTRA Synchrotron Light Source (Trieste, Italy). Spectra were collected at the sulfur K-edge (2485 eV) in fluorescence scan mode at a temperature of 100° K. EXAFS data reduction was performed using the Athena and Artemis softwares of the IFFEFIT package⁷. Statistical F-tests were applied to determine the statistical significance of different tested hypothesis.

3. Results and discussion

3.1. HEXD results

PDFs of natural felsöbányaite and of natural and synthetic basaluminite are shown in Figure 1 together with calculated PDFs of felsöbányaite⁴ along with its respective partial-PDFs (Al-Al, Al-O, Al-S, S-S, S-O and O-O atom pairs). PDFs of synthetic and natural basaluminite revealed that the synthesis process yields nanoparticles with similar local order than the natural samples. Particle size of both basaluminite types and of felsöbányaite were fitted with a size-function reproducing particles of spherical shape⁸. Basaluminite showed identical coherent domain sizes in both natural and synthetic samples, with a nanoparticle diameter of 1 nm, while the particle diameter obtained for the felsöbányaite sample was in the range of 4-5 nm. PDFs of both felsöbányaite and basaluminite exhibited similar structural features in the region between 1 and 6 \AA , with significant variations in peak intensities and width. Both basaluminite and felsöbányaite PDFs were compared in order to identify similarities and to associate individual peaks to interatomic distances using the calculated pair PDFs of felsobanyaite. The position of the first peak at 1.45 \AA corresponded to the S-O distance in the sulfate tetrahedron, whereas the second peak at 1.88 \AA was attributed to

the Al-O distance in the aluminum octahedron. The peak at 3 Å corresponded to the superposition of Al-Al and O-O distances, where Al-Al distance corresponded to edge-sharing aluminum octahedron and O-O distance was related to consecutive oxygen in the octahedron. The next three peaks (at 4, 4.8 and 6 Å) were associated with Al-O distances. Otherwise, the subsequent peaks at 6 Å presented low intensities, making it impossible to identify the corresponding atom pairs. According to the HEXD results, the basaluminite structure seems to have similar features to that of felsöbányaite, though with non-negligible distortions.

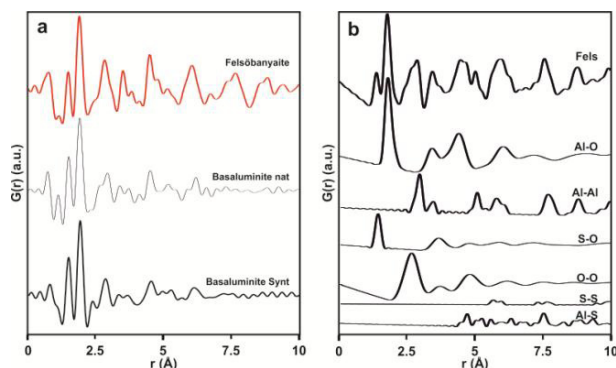


Fig. 1: (a) Natural felsöbányaite and natural and synthetic basaluminite PDFs and (b) theoretical and partial PDFs of felsöbányaite from the structure proposed by⁴.

3.2. S K-edge EXAFS

Sulfur K-edge EXAFS from synthetic and natural basaluminite, and the parameters of the different structural models tested are shown in Figure 2 and Table 1. Results from natural basaluminite were characterized by the presence of one shell at 1.45 ± 0.01 which is attributed to the S-O distance (Fig. 2b). This peak was consistent with an undistorted sulfate tetrahedron with coordination number of 5.12 ± 0.05 . A model where sulfate is forming an outer-sphere location yielded the best fit and a 75 % of confidence in the F-test, which is in agreement with the localization of sulfate in felsöbányaite⁴ (Table 1). On the other hand, S K-edge EXAFS in synthetic basaluminite showed that sulfate was retained by bidentate binucleate inner-sphere covalent ligands, where a double shell was identified with peaks located at 1.46 ± 0.01 Å and 3.02 ± 0.03 Å. These peaks were associated to S-O and S-Al distances with coordination number of 4.58 ± 0.05 and 2.00 (fixed value), respectively (Fig. 2b). The F-test values obtained for these models indicated that the bidentate binuclear inner-sphere was the best fit, where the confidence level was 70% (Table 1). The different structural positions observed in natural and synthetic basaluminite could be associated with the higher sulfate concentration in solution during the synthesis of basaluminite, where sulfate was placed in an outer-sphere location until this was fully occupied. From that point on, sulfate molecules could be retained in surface complexes with covalent bonds. The confidence levels obtained in both F-test studies were close to the minimum necessary, indicating that both models were possible and that the second shell was not clearly fitted.

Table 1: S k-edge EXAFS models for basaluminite.

Sample	Neighbor	N	σ^2	R	ΔE_0	V	$\Delta\chi^2$
Natural	One shell	5.119 ± 0.051	0.0004 ± 0.0002	1.453 ± 0.002	0.213 ± 1.320	4	16.3
Synthetic	Shell 1	4.583 ± 0.051	0.0009 ± 0.0003	1.458 ± 0.003	2.049 ± 1.201	5	17.9
	Shell 2	2.000 (fixed)	0.0057 ± 0.0037	3.017 ± 0.033	2.049 ± 1.201		

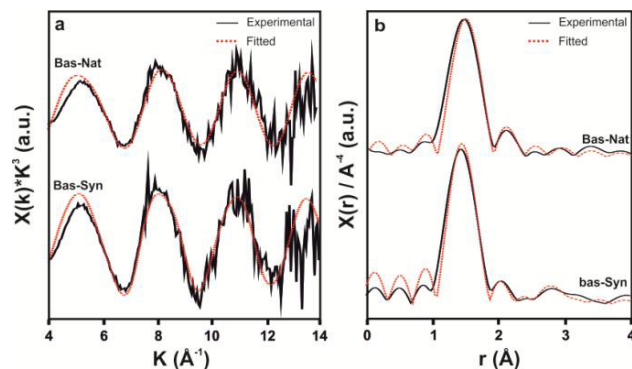


Fig. 2: (a) Amplitude part and (b) Fourier transform of K^3 -weighted EXAFS data at the S K-edge for natural and synthetic basaluminite. Experimental and fit curves are displayed in black and red color, respectively.

4. Conclusions

The previous consideration of basaluminite as nanocrystalline variety of felsöbányaite is discussed here. PDF results show that basaluminite has lower coherent domain size than felsobanyaite. In addition, disagreements between the two PDFs can be attributed to high levels of deformation in interatomic distances and bond angles. In both phases, aluminum octahedra form layers between which sulfate and water molecules reside. The basaluminite structure shows a high capacity to form surface complexes with sulfate, as indicated by the inner-sphere ligands observed in the S K-edge EXAFS. An accurate description of the sulfate bonding mechanisms has a strong environmental relevance, due to anionic exchange processes that could be at play in AMD-affected streams and ASS. These processes have strong implications in the mobility of contaminants. This preliminary work evidences the need for in-depth structural analyses that allow determining precisely local order characteristics of basaluminite.

Acknowledgements

We would like to thank the Regional Government of Andalucía (Spain; P12-RNM-2260), the Spanish Ministry of Economic and Competitiveness (EMPATIA, CGL2013-48460-C2-R) and a grant from Labex OSUG@2020 (investissements d'avenir – ANR10 LABX56) for financial research support. The authors are very grateful to the ESRF (ID31 beamline) and ELETTRA (XAFS beamline) personnel for their assistance during our experiment (20145106).

References

1. Nordstrom, D. K. The effect of sulfate on aluminum concentrations in natural waters: some stability relations in the system Al_2O_3 - SO_3 - H_2O at 298 K. *Geochim. Cosmochim. Acta* **46**, 681–692 (1982).
2. Bigham, J. M. & Nordstrom, D. K. Iron and aluminum hydroxysulfates from acid sulfate waters. *Rev. Mineral. Geochemistry* **40**, 351–403 (2000).
3. Carrero, S. et al. The potential role of aluminium hydroxysulphates in the removal of contaminants in acid mine drainage. *Chem. Geol.* **417**, 414–423 (2015).
4. Farkas, L. & Pertlik, F. Crystal structure determinations of felsöbányaite and basaluminite, $Al_4(SO_4)(OH)_{10} \cdot 4H_2O$. *Acta Mineral. Szeged* **38**, 5–15 (1997).
5. Gilbert, B., Huang, F., Zhang, H., Waychunas, G. A. & Banfield, J. F. Nanoparticles: strained and stiff. *Science* **305**, 651–654 (2004).
6. Farrow, C. L. et al. PDFgui user guide. (2009).
7. Ravel, B. & Newville, M. ATHENA, ARTEMIS, HEPHAESTUS: Data analysis for X-ray absorption spectroscopy using IFEFFIT. *J. Synchrotron Radiat.* **12**, 537–541 (2005).
8. Gilbert, B. Finite size effects on the real-space pair distribution function of nanoparticles. *J. Appl. Crystallogr.* **41**, 554–562 (2008).